Optics Communications 283 (2010) 4122–4125

Contents lists available at ScienceDirect

Optics Communications

journal homepage: www.elsevier.com/locate/optcom

Multilayered scattering reference mirror for full field optical coherence tomography with application to cell profiling

Rony Sharon, Ron Friedman, I. Abdulhalim *

Department of Electro-Optic Engineering, Ben Gurion University, Beer Sheva 84105, Israel

ARTICLE INFO

Article history:
Received 11 December 2009
Received in revised form 30 April 2010
Accepted 25 May 2010

ABSTRACT

A multilayered scattering structure is proposed and demonstrated as a reference mirror for use with full field optical coherence tomography (FF-OCT) to increase contrast of tissue imaging and provide compensation. Common-path FF-OCT systems were built demonstrating high resolution cell profiling. The use of this mirror with frequency domain FF-OCT allows 3D images in real time.

© 2010 Elsevier B.V. All rights reserved.

Optical coherence tomography (OCT) technique has revolutionized biomedical optical imaging in several areas such as opthalmoscopy, dermatology, endoscopy and cardiology [1]. The frequency domain (FD) OCT allows in depth sectional imaging without axial scanning while full field (FF) OCT allows topographic imaging without lateral scanning. The ability of OCT to give 3D images in real time without any scanning can be conceptually achieved by combining FD-OCT with FF-OCT. The only remaining scan is the spectral scan, which can be attained fast enough using tunable lasers and tunable filters. Two problems are awaiting solution however to achieve this goal: the first is the limitation on the depth of focus (DoF) of the lenses or microscope objectives used in FF-OCT and the second is the reference path compensation required when imaging deep tissue layers. The problem of extending the DoF in OCT in general and in FF-OCT in particular is being attacked by different approaches such as: the use of axicons [2–4], annular lenses [5], inverse scattering [6], and image processing [7–9]. The problem of compensating for the refractive index mismatch between the reference and sample paths was attacked by the use of retroreflector in the reference arm [10], dynamic focusing [11], and digital techniques [12,13]. In this article we propose and demonstrate the use of scattering multilayered mirror (SMM) to both help in compensation and partially overcome the depth of focus limitation. High resolution cell profiling is demonstrated using FF-OCT system combined with the SMM in the reference path.

The concept of the SMM is illustrated in Fig. 1 which consists of a stack of transparent layers and scattering interfaces between the transparent regions. Ideally we would like to have the interfacial scattering layers thicknesses d_s to be as small as possible but not much smaller than the wavelength. The amplitude reflectivity function of the structure may then be described by the following:

$$r_{SMM} = r_0 + \sum_{j=1}^{N} r_j \exp(i2\omega P_j / c) \tag{1}$$

where here r_0 is the reflectivity coefficient from the first non-scattering interface and r_j is that of scattering interface number j that includes in it the random phase attained upon scattering. The optical pathlength is that due to single pass travel through the layers and it is given by: $P_j = \sum_{m=1}^{j} n_m z_m$ where n_m and z_m are the refractive indices of the layers and the locations of the interfaces respectively. In the ideal case one would like to avoid any correlations between the interfacial reflections so that multiple interferences are avoided i.e., $\langle r_j r_{j'} \rangle = |r_j r_{j'}| \delta_{jj'}$ where $\delta_{jj'}$ is the Kronecker delta function. In this case the total absolute reflectivity is given as an incoherent sum: $|r_{SMM}|^2 \approx \sum_{j=0}^{N} |r_j|^2$. Now assuming a layered biological object made of M scattering layers with its scattering function described by similar form to Eq. (1):

$$r_{ob} = r_{0ob} + \sum_{l=1}^{M} r_{ob-l} \exp(i2\omega P_{ob-l} / c) \tag{2}$$

where here the optical pathlength is that due to single pass travel through the sample layers and given by: $P_{ob-l} = \sum_{q=1}^{l} n_q z_q$ with n_q, z_q being the refractive indices of the layers and the locations of the interfaces respectively. The interference signal at frequency ω will then be given by the following:

$$I(\omega, P_{ob-l}, P_j) = S(\omega)\left\{|r_{SMM}|^2 + |r_{ob}|^2\right\} + 2\mathrm{Re}\left\{\sum_{j,l}^{N,M} |r_j^* r_{ob-l}| S(\omega) \exp(i2\omega(P_{ob-l} - P_j)/c + i\delta\varphi_s)\right\} \tag{3}$$

* Corresponding author.
E-mail address: abdulhlm@bgu.ac.il (I. Abdulhalim).

0030-4018/$ – see front matter © 2010 Elsevier B.V. All rights reserved.
doi:10.1016/j.optcom.2010.05.047

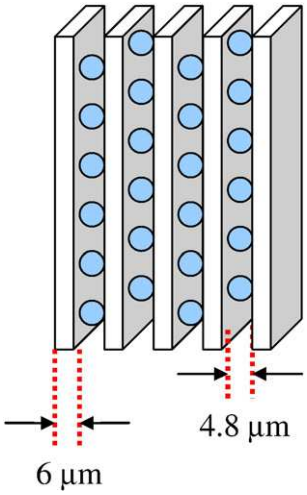

Fig. 1. Schematic side view of the multilayered diffusive mirror.

where here $S(\omega)$ is the source function and $\delta\varphi_s$ is any additional phase difference that can contribute to the interference signal. In the time domain OCT (TD-OCT) the integration over the whole spectral range leads to interferograms centered at the pathlengths: $P_{oj-l}=P_j$ if $\delta\varphi_s$ is ignored. Hence without any axial scanning the multilayered scattering reference mirror allows obtaining interferograms centered at the locations of the sample layer interfaces. The mirror will operate best when the number of layers and their locations are similar in both the reference and the sample. To avoid this limitation the reference mirror should be designed such that the layer thicknesses are less than half the coherence length. Then assuming the sample layers are thicker than the coherence length, interferograms will be obtained only at the locations of the sample layers. Hence the design will be optimum if there is an a priori knowledge on the sample layered structure.

The SMM shown schematically in Fig. 1 is composed of several layers of mylar sheets, each 6 μm thick and in between each two there is a layer of silica microspheres 4.8 μm thick embedded in UV glue Norland NOA 68. The microspheres with the UV glue with 14% concentration were mixed together in an ultrasound path to prevent aggregation of the silica spheres. The stack was then prepared layer by layer by shining UV light on the microspheres-glue mixture between two mylar sheets. While scanning a certain tissue the refractive index in the sample is different from the one in the reference arm, causing a small difference in the optical path between the two arms that leads to a difference in the contrast and a need to move the reference arm in order to match the optical path of the two arms. Moving the reference arm will cause a defocus in the system. This unique multilayered mirror allowed us to compensate the focus in the reference arm without any mechanical movement. This is done by focusing on a different layer within the mirror structure at a location that matches the optical path of the sample arm. A note should be added on the size and concentration of the microspheres used as their choice and contrast between their refractive index and the glue material determines the amount of scattering and its characteristics. One can design such structure depending on the application so that the reflection characteristics of the SMM become as close as possible to those of the sample to be inspected.

A "nearly" common-path full field OCT system was built based on Michelson type interferometer as shown in Fig. 2. The relatively short arms made this configuration more stable than the Linnik configuration. The system was built on an optical bench without a need for vibration isolation, which is why we called it "nearly" common-path FF-OCT system. The Mirau interferometer is usually referred to as common path but in fact it is also only "nearly" common path however it is more stable because the reference mirror is fixed within the Mirau objective. The lack for scanning the reference mirror in the Mirau case is a disadvantage as it does not allow compensation and limits its use to thin objects [5]. These are the reasons which led us to build the Michelson type interference microscope. To minimize aberrations effects we used an achromatic triplet Hastings lens (Edmunds NT30-229) as an objective corrected for

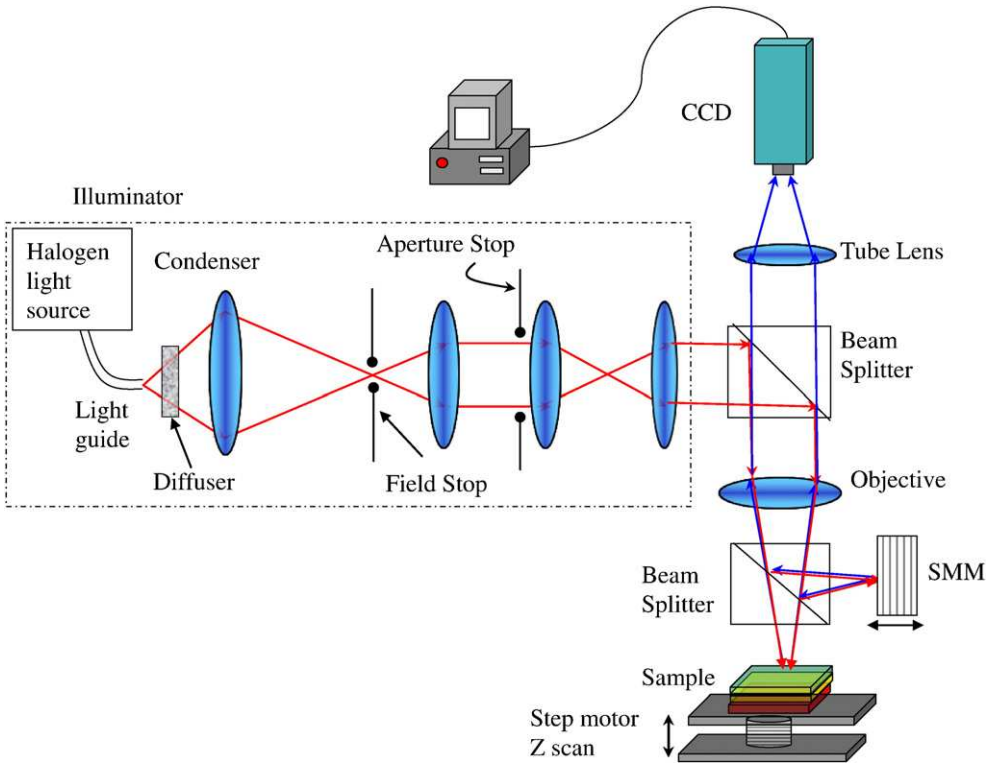

Fig. 2. Schematic layout of the experimental setup.

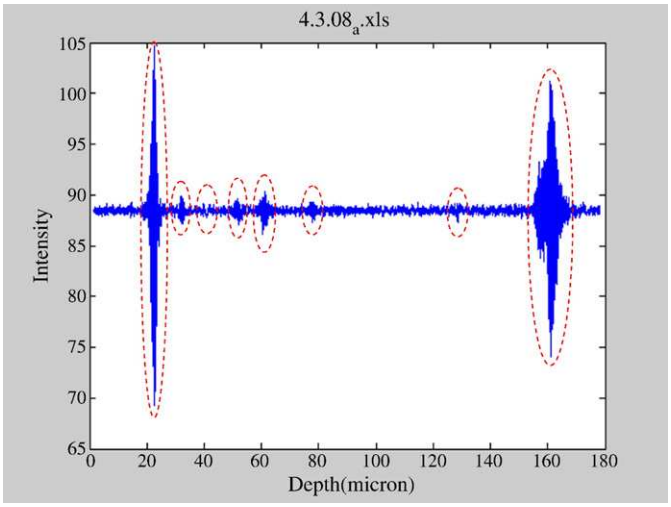

Fig. 3. Interferogram obtained from the SMM against a plan mirror in the sample arm.

spherical, distortion and chromatic aberrations for the visible range of the spectrum and has large working distance. A halogen lamp source was used to provide wide spectral bandwidth together with Kohler uniform illumination built in-house. The sample was positioned on a stage connected to a step motor with 20 nm resolution controlled by a computer and the images were captured by a CCD camera during the *Z* scan. The sample arm of the interferometer contained the sample substance, and the reference arm contained the unique diffusive multilayered mirror (SMM). By performing *Z* scan of the sample arm we obtained enface 3-D tomographic images.

The mirrors were aligned first to obtain a spatial fringe size larger than the size of the field of view. This is usually termed "infinite fringe" case in the jargon of interference microscopy. In Fig. 3, a *Z* scan showing all the interfaces of the multilayered mirror when in the sample arm there was a plan mirror. Note that the inner interfaces exhibit much lower signal than the first and last interfaces as expected since the inner layers are diffusive and the contrast in the refractive indices is much lower, however when tissue is imaged these inner surfaces are important in revealing information on the inner structure of the sample. One can choose a different separation material to give larger refractive index contrast with the diffusing layer and as mentioned above to optimize the microspheres so that the signal from the inner layers is higher. In Fig. 4 two scans of onion epidermis are shown, the first one (left lower) was conducted with a regular reference mirror and no compensation in the reference arm, where one can see the difference in amplitude between the first and the second interface of the epidermis due to the movement of the coherence plane. The second scan (right lower) was conducted with the same epidermis but having the multilayered mirror in the reference arm without any compensation, showing clearly that both interfaces exhibit the same signal amplitude. Note that in the calculation of the layer thickness we assumed a refractive index of the SMM layers of 1.55, thus giving a thickness of 44 μm not far from the nominal value. The difference from the reported value without the SMM (bottom left) is about 10% which could be due to some water loss of the onion layer during the experiment that causes the effective thickness to decrease. The additional peaks in the interferogram with lower amplitude (dashed arrows) are indicative of an internal onion epidermis profile which could not be observed without the SMM.

Due to the small interferometer arms, the FF-OCT system was very stable exhibiting similar stability to the common-path Mirau

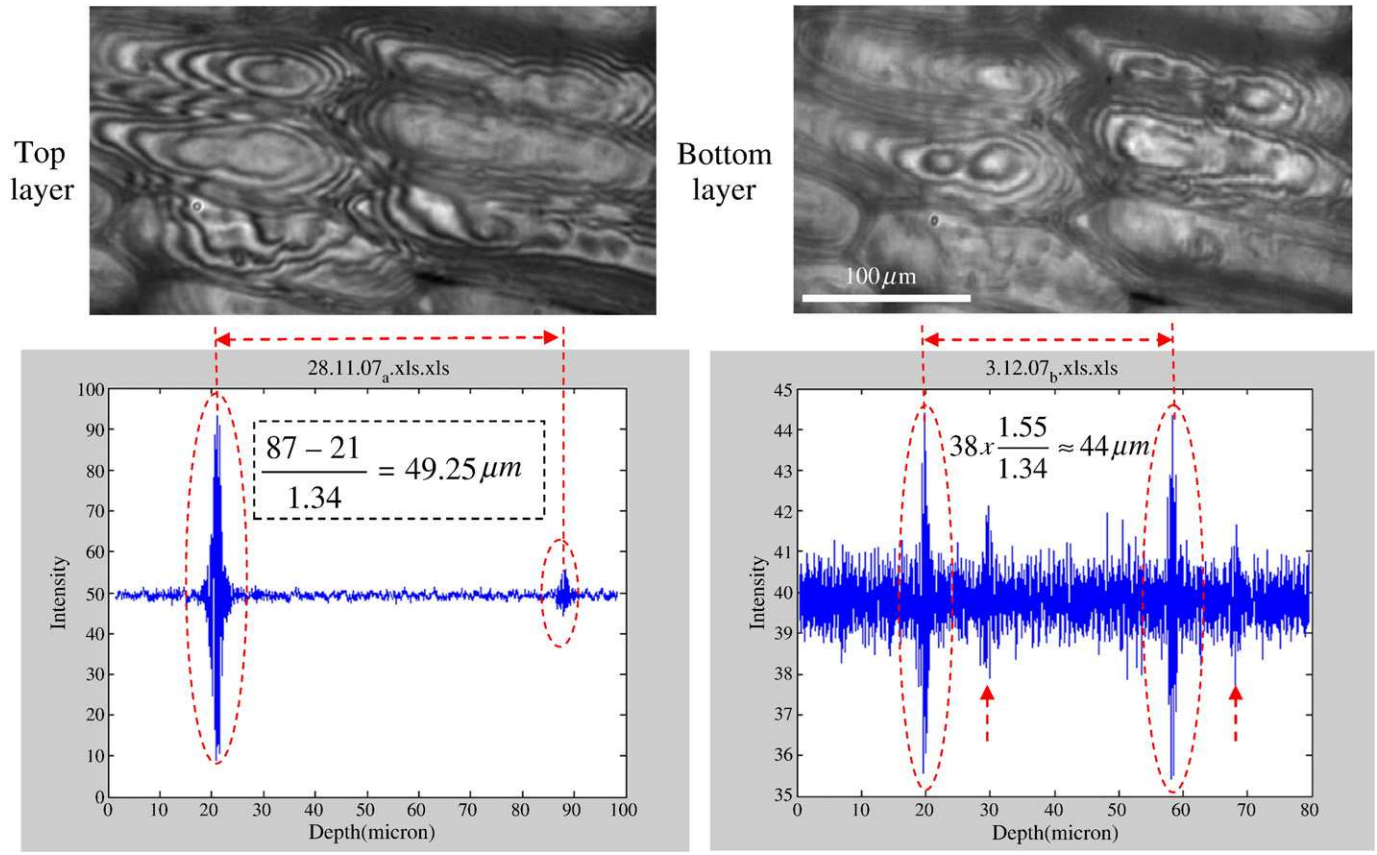

Fig. 4. Top pictures show interference images of the top and bottom of onion epidermis. Lower left is the *Z* scan interferogram obtained without the SMM while the lower right is with the SMM as reference mirror. The dashed arrows in the bottom right image indicate some weak signals that originate from the fact that the epidermis has some internal profile, not seen without the SMM. This is clear evidence that the inner interfaces of the SMM mirror can provide information on the internal structure of the sample and not only its outer surfaces.

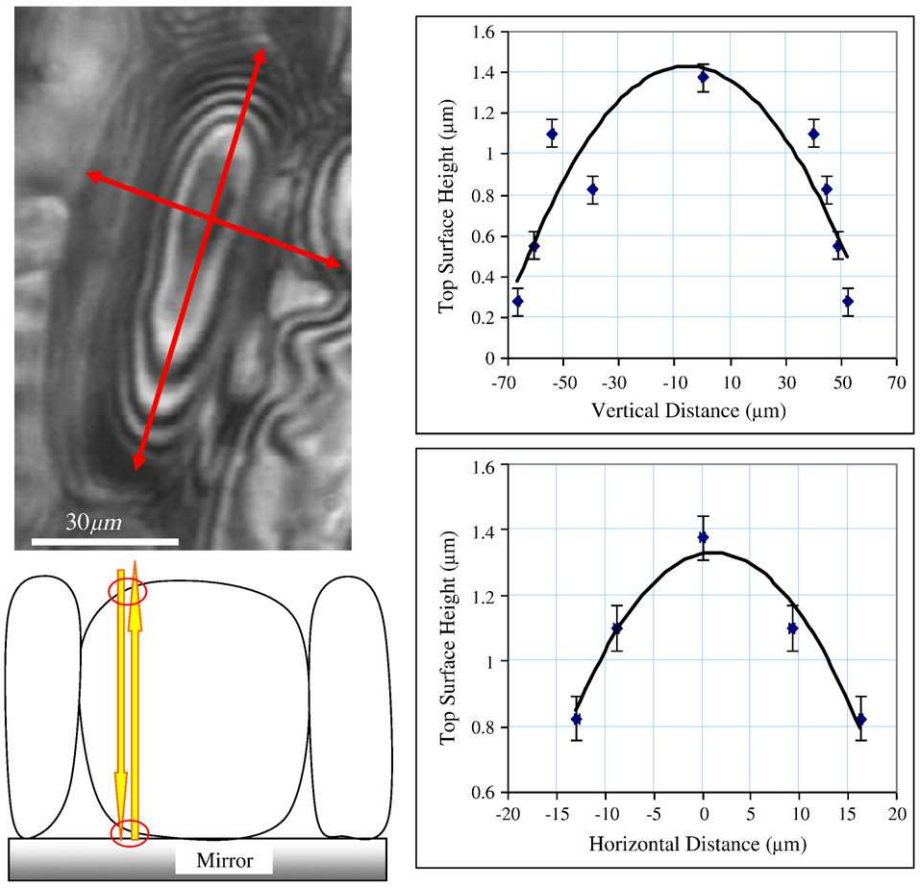

Fig. 5. The interferometric picture (top left) is showing one single cell and the arrows indicate the directions of the calculated profiles shown in the right hand side. The bottom left is a schematic model for the non-spherical cell profile which is caused partially by the fact that the cells are adhered to a plan mirror surface and touching each other.

interferrometric microscope. Using this latter system, we have demonstrated cell profiling recently [5,14], however due to the fact that the reference mirror is inside the Mirau objective, it was not possible to perform any scan compensation. Also it was not possible to block the reference beam in order to check whether the interference fringes were a result of multiple interferences within the onion cell combined with some lensing effects or it is a result of interference between the two interferometer arms.

The system reported in this article avoids this limitation and provides a clear proof that cell profiling is possible using two beams interferometry. Onion epidermis was successfully imaged both in the lateral and axial directions and the average epidermis thickness was measured: ~44 μm (good correlation with literature reference ~45 μm). In Fig. 5, onion epidermis cell profiling is demonstrated where each fringe cycle corresponds to a height variation of 275 nm. The error bars correspond to one quarter of a fringe size. The fringe size is well known to be affected by the coherence and other parameters of the interference microscope, in our case it is measured experimentally from the plane mirror interferogram [15,16]. Assuming the cell has symmetrical wall profile we could reconstruct the cell profile from the recorded image as shown in Fig. 5 along the cell major axes. It is possible that the onion epidermis cells have non-spherical profile, but shape distortions can also occur while handling these cells and assembling them on the reflecting surface of the planar mirror. The continuous lines are parabolic fits to the experimental points. It should be addressed that the SMM allows also observing some internal structured profile as can be noticed from the signals designated by the dashed arrows in the bottom right of Fig. 4.

To conclude we have designed, built and demonstrated diffusive multilayered mirror for optical coherence tomography and used it with full field OCT setups. This mirror allows compensation for the index mismatch between the tissue sample arm and the reference arm and it helps maintaining focused images without the need for dynamic focusing. This mirror allows surface profiling without scanning both for the external and for other internal profiles of the structure as long as the structure is within the depth of focus.

References

[1] B.E. Bouma, G.J. Tearney (Eds.), Handbook of Optical Coherence Tomography, Marcel Dekker, New York, 2002.
[2] Z.H. Ding, H.W. Ren, Y.H. Zhao, J.S. Nelson, Z.P. Chen, Opt. Lett. 27 (2002) 243.
[3] R.A. Leitgeb, M. Villiger, A.H. Bachmann, L. Steinmann, T. Lasser, Opt. Lett. 31 (2006) 2450.
[4] K. Lee, J.P. Rolland, Opt. Lett. 33 (2008) 1696.
[5] I. Abdulhalim, Ron Friedman, Lior Liraz, Ronen Dadon, Proc. SPIE 6627 (2007) 662719.
[6] T.S. Ralston, D.L. Marks, P.S. Carney, S.A. Boppart, J. Opt. Soc. Am. A 23 (2006) 1027.
[7] M.D. Kulkarni, C.W. Thomas, J.A. Izatt, Electron. Lett. 33 (1997) 1365.
[8] A. Podoleanu, I. Charalambous, L. Plesea, A. Dogariu, R. Rosen, Phys. Med. Biol. 49 (2004) 1277.
[9] Y. Yasuno, J.I. Sugisaka, Y. Sando, Y. Nakamura, S. Makita, M. Itoh, T. Yatagai, Opt. Express 14 (2006) 1006.
[10] J.M. Schmitt, S.L. Lee, K.M. Yung, Opt. Commun. 142 (1997) 203.
[11] A. Dubois, G. Moneron, C. Boccara, Opt. Commun. 266 (2006) 738.
[12] A.F. Fercher, C.K. Hitzenberger, M. Sticker, R. Zawadzki, Opt. Express 9 (2001) 610.
[13] Maciej Wojtkowski, Vivek Srinivasan, Tony Ko, James Fujimoto, Andrzej Kowalczyk, Jay Duker, Opt. Express 12 (2004) 2404.
[14] Ron Friedman, "FULL FIELD AND COMMON PATH OPTICAL COHERENCE TOMOGRAPHY SYSTEM", M.Sc thesis, Ben Gurion University of the Negev (2007).
[15] I. Abdulhalim, J. Mod. Opt. 48 (2001) 279.
[16] I. Abdulhalim, J. Opt. A: Pure Appl. Opt. 8 (2006) 952.